









## ORIGINAL ARTICLE

# Efficacy and toxicity of hydrogen peroxide producing electrochemical bandages in a porcine explant biofilm model

Gretchen Tibbits<sup>1</sup>  | Abdelrhman Mohamed<sup>1</sup>  | Suzanne Gelston<sup>1</sup>  |  
Laure Flurin<sup>2</sup>  | Yash S. Raval<sup>2</sup>  | Kerryl Greenwood-Quaintance<sup>2</sup>  |  
Robin Patel<sup>2,3</sup>  | Haluk Beyenal<sup>1</sup> 

<sup>1</sup>The Gene and Linda Voiland School of Chemical Engineering and Bioengineering, Washington State University, Pullman, Washington, USA

<sup>2</sup>Division of Clinical Microbiology, Mayo Clinic, Rochester, Minnesota, USA

<sup>3</sup>Division of Public Health, Infectious Diseases and Occupational Medicine, Mayo Clinic, Rochester, Minnesota, USA

## Correspondence

Haluk Beyenal, The Gene and Linda Voiland School of Chemical Engineering and Bioengineering, Washington State University, Pullman, WA, USA.

Email: [beyenal@wsu.edu](mailto:beyenal@wsu.edu)

## Funding information

National Institutes of Health, Grant/Award Number: R01AI091594

## Abstract

**Aims:** Effects of H<sub>2</sub>O<sub>2</sub> producing electrochemical-bandages (e-bandages) on methicillin-resistant *Staphylococcus aureus* colonization and biofilm removal were assessed using a porcine explant biofilm model. Transport of H<sub>2</sub>O<sub>2</sub> produced from the e-bandage into explant tissue and associated potential toxicity were evaluated.

**Methods and Results:** Viable prokaryotic cells from infected explants were quantified after 48 h treatment with e-bandages in three *ex vivo* *S. aureus* infection models: (1) reducing colonization, (2) removing young biofilms and (3) removing mature biofilms. H<sub>2</sub>O<sub>2</sub> concentration-depth profiles in explants/biofilms were measured using microelectrodes. Reductions in eukaryotic cell viability of polarized and nonpolarized noninfected explants were compared. e-Bandages effectively reduced *S. aureus* colonization ( $p = 0.029$ ) and reduced the viable prokaryotic cell concentrations of young biofilms ( $p = 0.029$ ) with limited effects on mature biofilms ( $p > 0.1$ ). H<sub>2</sub>O<sub>2</sub> penetrated biofilms and explants and reduced eukaryotic cell viability by 32–44% compared to nonpolarized explants.

**Conclusions:** H<sub>2</sub>O<sub>2</sub> producing e-bandages were most active when used to reduce colonization and remove young biofilms rather than to remove mature biofilms.

**Significance and Impact of Study:** The described e-bandages reduced *S. aureus* colonization and young *S. aureus* biofilms in a porcine explant wound model, supporting their further development as an antibiotic-free alternative for managing biofilm infections.

## KEYWORDS

biofilm, electroceutical, electrochemical bandage, hydrogen peroxide, porcine explant, *Staphylococcus aureus*

This is an open access article under the terms of the [Creative Commons Attribution-NonCommercial](https://creativecommons.org/licenses/by-nc/4.0/) License, which permits use, distribution and reproduction in any medium, provided the original work is properly cited and is not used for commercial purposes.

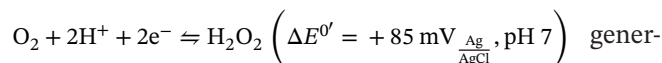
© 2022 The Authors. *Journal of Applied Microbiology* published by John Wiley & Sons Ltd on behalf of Society for Applied Microbiology.

## INTRODUCTION

It was estimated that in 2014 ~8.2 million people suffered from chronic wounds in the United States (Sen, 2019). A wound that has not progressed through the normal healing stages is categorized as chronic and is often plagued with repeated infection (Sen, 2019). Such wound infections are characteristically difficult to treat and often require both antibiotic therapy and physical debridement. Chronic wound infections frequently harbour micro-organisms in a biofilm form, in which an extracellular matrix is present, aiding in bacterial survival and tolerance to stresses. The structure and chemical microenvironment of a biofilm aid pathogen survival, delay wound healing, and hinder antibiotic treatment efficacy (Dowd et al., 2011; Metcalf & Bowler, 2013; Percival et al., 2012). Biofilms tolerate 10–1000 times higher concentrations of many antibiotics than do planktonic bacteria (Gupta et al., 2016; Uruen et al., 2021). Effective management of biofilms formed on wound surfaces could promote wound healing.

Antibiotics are a strategy for removing biofilms from infected wounds. However, extracellular polymeric substance (EPS) in biofilms restricts the activity of some antibiotics by limiting transport into the biofilm (Anderl et al., 2000; Stewart, 1996), providing sites for interactions with and absorption to biomolecules to EPS (Davenport et al., 2014), supporting cell-to-cell communication (Shrout et al., 2011), and contributing to intrinsic antibiotic tolerance (Høiby et al., 2011). As biofilms grow, maturity leads to coordinated quorum sensing and signalling pathways, exosome cell-to-cell communication (Kowal et al., 2014; Valadi et al., 2007), extracellular DNA (Devaraj et al., 2019), and increased cell numbers. Communication pathways allow cells to signal environmental changes and activate survival mechanisms. Therefore, it is expected that mature biofilms would be more resistant to antibiotics or biocides.

Natural biocides are products of host immune response to infection and as such, wound healing (Halliwell, Clement, & Long, 2000; Hampton et al., 1998). A common biocide is hydrogen peroxide ( $H_2O_2$ ). The use of  $H_2O_2$  in the treatment of wound biofilms is hampered by its short half-life, instability in wound beds, and toxicity to host tissue when used at high concentrations ( $>50 \mu\text{mol L}^{-1}$ , depending on the exposure location) (Halliwell, Clement, & Long, 2000). Our team is developing an electrochemical system for continuous generation of  $H_2O_2$  for prevent and treating wound infections (Raval et al., 2019, 2020; Sultana et al., 2015).  $H_2O_2$  is an oxidizing agent that causes membrane depolarization, oxidizes proteins and inhibits enzyme activity, resulting in cell death (Finnegan et al., 2010). The electrochemical system continuously generates  $H_2O_2$  from partial reduction of dissolved oxygen through the reaction,



ated at  $0.085 V_{\frac{Ag}{AgCl}}$  (Allen J. Bard, 2001; Sultana et al., 2015). An electrochemical scaffold (e-scaffold) prototype, which allowed facile study of electrochemical reactions, reduced *in vitro* biofilms and explant biofilms in liquid media (Raval et al., 2019, 2020; Sultana et al., 2015, 2016). Substitution of a hydrogel for the liquid medium was used to transform e-scaffolds into electrochemical bandages (e-bandages) for direct application to wound surfaces. The e-bandage reduced *in vitro* biofilms of mono- and dual-species micro-organisms, including methicillin-resistant *S. aureus*, multidrug-resistant *A. baumannii* and yeast (Mohamed et al., 2021; Raval et al., 2022; Raval, Mohamed, et al., 2021).

As a result of their low cost, high accessibility and structural similarity to the human dermis, porcine explants are utilized as a model for wound healing, assessing wound biofilms and treatment efficacy (Sullivan et al., 2001). *Ex vivo* porcine models have been used to study bacterial-tissue interactions (Roberts et al., 2019; Yang et al., 2013), activity of antimicrobial agents (Lone et al., 2015; Phillips et al., 2015; Roberts et al., 2019; Roche et al., 2019; Yang et al., 2017) and cytotoxicity of treatments (Sultana et al., 2015). Here, porcine explants were used to study the efficacy, toxicity and transport of  $H_2O_2$  produced by e-bandages. Microbial colonization, alongside young and mature biofilm removal were tested.

## MATERIALS AND METHODS

### $H_2O_2$ producing e-bandage

Construction and preparation of the  $H_2O_2$  producing e-bandage was performed as previously described (Mohamed et al., 2021). The e-bandage is a three-electrode system consisting of a conductive carbon fabric (Zoltek, Panex 30 PW-06) as the working and counter electrode, and an Ag/AgCl reference wire.  $H_2O_2$  is produced as a result of oxygen reduction on the working electrode of the e-bandage. When the e-bandage was applied to biofilms, the working electrode always faced toward the biofilm. Titanium wires (TEMCo, Amazon.com, catalogue #RW0524) were connected to the working and counter electrodes using nylon sew snaps (Dritz, item #85). A Gamry Interface 1000 potentiostat connected with a Gamry ECM8 electrochemical multiplexer (Gamry Instruments) was used to polarize the working electrode at  $-0.6 V_{\frac{Ag}{AgCl}}$  to generate  $H_2O_2$ . Before use, e-bandages were autoclaved (15 min at  $121^\circ\text{C}$ ).

## Chemicals, supplies and bacteria

Dulbecco's Modified Eagle Medium (DMEM) (Thermo Fisher Scientific, #21063029) and 100× antibiotic-antimycotic (10,000 units ml<sup>-1</sup> penicillin, 10,000 µg ml<sup>-1</sup> streptomycin and 25 µg ml<sup>-1</sup> amphotericin B, ThermoFisher, cat. no. 15240096), and tryptic soy broth (TSB, BD Ref. 211825) were used as purchased. Phosphate buffer saline (PBS) solution contained 0.01 mol L<sup>-1</sup> Na<sub>2</sub>HPO<sub>4</sub>, 1.8 mmol L<sup>-1</sup> KH<sub>2</sub>PO<sub>4</sub>, 0.137 mol L<sup>-1</sup> NaCl and 2.7 mmol L<sup>-1</sup> KCl, and was autoclaved prior to use (15 min at 121°C). Hydrogel was prepared by dissolving 1.8 wt% sterile xanthan gum (Namaste Foods LLC) in 500 ml of sterile PBS. Three types of tryptic soy agar (TSA, BD Ref. 236950) plates were used. 1.8 wt% TSA was used for CFU quantification before and after treatments, 1× antimicrobial agent (10 units ml<sup>-1</sup> penicillin, 10 µg ml<sup>-1</sup> streptomycin and 0.025 µg ml<sup>-1</sup> amphotericin B) TSA plates for cell viability measurements, and 0.1× antimicrobial agent (1 unit ml<sup>-1</sup> penicillin, 1 µg ml<sup>-1</sup> streptomycin and 0.0025 µg ml<sup>-1</sup> amphotericin B) TSA plates for infection experiments. 700 ml of 1.8 wt% TSA was autoclaved and allowed to cool to 45°C. 1× and 0.1× plates were prepared by adding 200 µl or 20 µl of stock antimicrobial agent solution, respectively, to 20 ml of TSA and poured into individual Petri dishes. When not in use, TSA plates were stored at 4°C. A clinical isolate of methicillin-resistant *S. aureus* (IDRL-6169) was used for all experiments.

## e-Bandage assessments

e-Bandages were tested to assess efficacy and toxicity of H<sub>2</sub>O<sub>2</sub> and transport of H<sub>2</sub>O<sub>2</sub> into explants (Figure 1). Three *S. aureus* infection models were used—colonization, and young and mature biofilms—to quantify antimicrobial effects; noninfected explants used to study toxicity. All treatment durations were 48 h and all experiments included polarized and nonpolarized e-bandages and no e-bandage. For infection colonization experiments, explants were inoculated with *S. aureus* and treatment started right away. Young biofilms were allowed to establish for 24 h before starting treatment; mature biofilms were allowed to establish for 3 days before starting treatment. Eukaryotic cell toxicity was assessed absent infection.

## Explant agar biofilm model

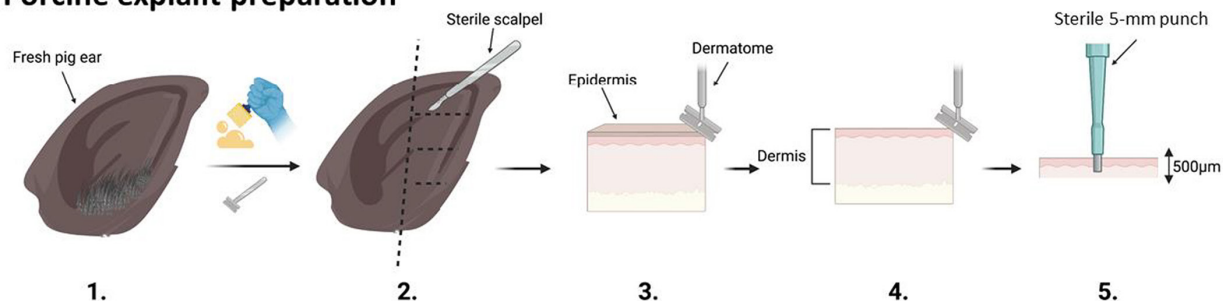
The experimental procedure is summarized in Figure 1. Infected and noninfected models of porcine explants began with surgically scrubbing (Figure 1.1) and shaving off hair from a fresh pig ear (Figure 1.2). The outer edge

of the ear was cut off with a sterile scalpel (Figure 1.3) and the epidermis layer removed with a sterile Padgett's dermatome (Nouvag TCM 3000) (Figure 1.4). A 500-µm slice of the dermis was cut. Then, a 5-mm biopsy punch (Robbins Instruments Part No. RBP-50) was used to punch 5-mm sections of the tissue (Figure 1.5). For the noninfected model (Figure 1.6A), a 5-mm explant was placed onto a 13-mm polycarbonate membrane (Cytivia Life Sciences, 10417001) on a 1× antimicrobial agent TSA plate (Figure 1.7A). 100 µl of hydrogel was added to the explant. Then the e-bandage was soaked in PBS and 100 µl of hydrogel added inside the e-bandage. The e-bandage was placed on the noninfected explant, and 100 µl of hydrogel added on top of the e-bandage (Figure 1.8A). The e-bandage was covered with Tegaderm™ (3M, 16002) and connected to a potentiostat to operate the e-bandage, and (Figure 1.9A) finally a PrestoBlue cell viability assay (ThermoFisher, cat. no. A13261) was performed after treatment. For the infected model (Figure 1.6B) a 5-mm explant was placed onto a 13-mm polycarbonate membrane on a 0.1× antimicrobial agent TSA plate and inoculated with bacteria (Figure 1.7B) and 100 µl of hydrogel was added on top of the infected explant. The e-bandage was soaked in PBS, 100 µl of hydrogel added to the inside layers of the e-bandage, the e-bandage placed on top of the infected explant, and 100 µl of hydrogel added on top of the e-bandage. (8B) The e-bandage was covered with Tegaderm™ and connected to a potentiostat to operate the e-bandage, and finally (9B) quantification of biofilm was done by serial dilution after treatment. The detailed protocol can be found in SI Section 3 (Detailed Explant Preparation Protocol).

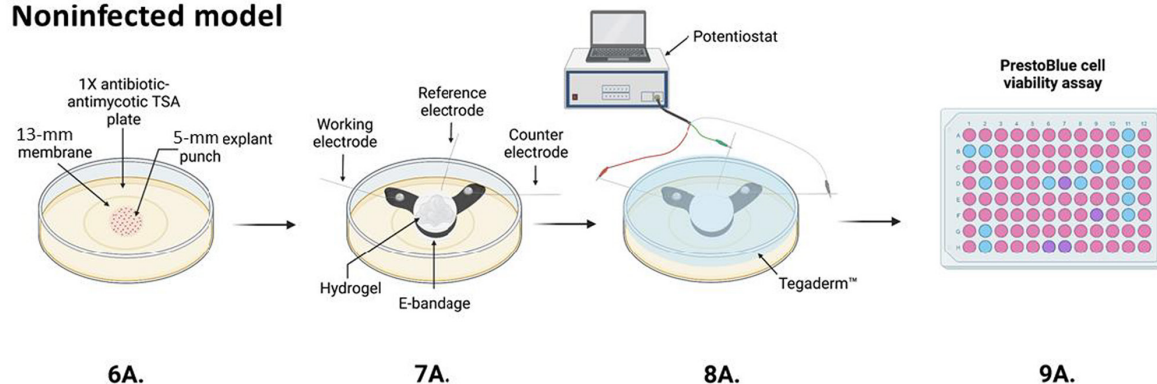
## Porcine explant preparation

Porcine explant preparation was modified from previous explant models to accommodate an agar model (Zmuda et al., 2020). Ear tissue was harvested from fresh pigs (same day) from local butchers, immediately cooled to 4°C and transported to the laboratory for processing. The ears were scrubbed with a single-use sponge and 10% detergent under cold water (Figure 1.1). Next, the hair was removed using an electric razor and the ears rinsed with cold water. The ears were then scrubbed with betadine soap for 10 min using gauze sponges and sprayed with 70% ethanol. The ears were then placed on UV-sterilized aluminium foil in a biosafety cabinet and cleaned again using betadine solution and sterile gauze sponges for 5 min. Betadine was removed using 70% ethanol-soaked gauze sponges. This step was continued until the gauze sponges could be wiped across the surface with no discoloration of the sponge. The outer rim of the ear was

## Porcine explant preparation



## Noninfected model



## Infected model

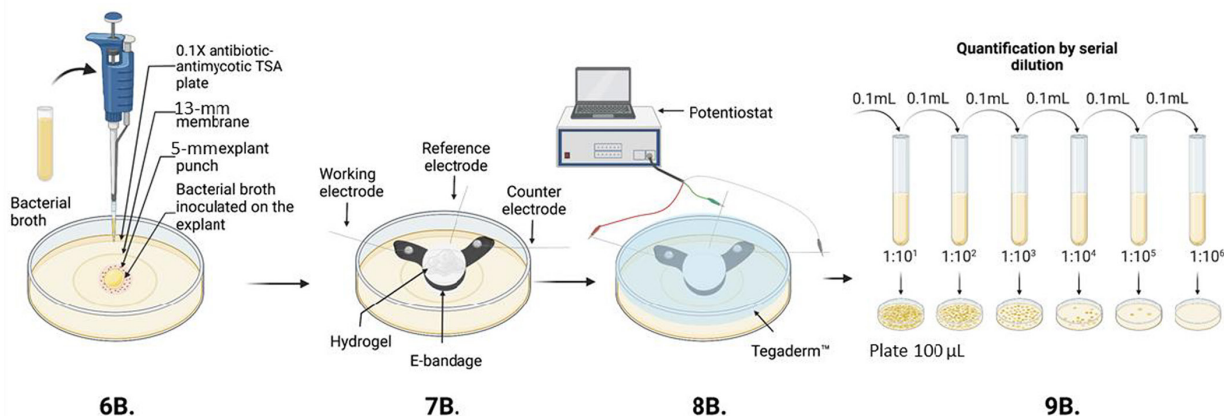


**FIGURE 1** Schematic of porcine explant preparation (1–5), noninfected model (6A–9A), and infected model experiments (6B–9B), e-bandage applications and treatment (7A, 8A, 7B, 8B), colony-forming unit quantification (9B), and PrestoBlue cell viability assay (9A). Images prepared using BioRender®.

then removed using a single-use sterile razor blade and cut into three or four pieces (Figure 1.2). The epidermis was removed using a dermatome set to 500µm and discarded (Figure 1.1–3). A 500-µm layer of the dermis was removed using the dermatome for a 500-µm-thick tissue (Figure 1.1–4). The tissue was placed in sterile DMEM in a Petri dish. The 500-µm dermis tissue was then punched with a 5-mm sterile biopsy punch (Figure 1.1–5). A UV-sterilized 13-mm, 0.2-µm pore-size membrane was placed on a 1× antimicrobial agent TSA plate (cell viability) or 0.1× antimicrobial agent TSA plate (infection models) and the 5-mm porcine punch positioned in the centre of the membrane. The infected and noninfected explants were

maintained in an incubator with 5% CO<sub>2</sub>, 95% air and 95% relative humidity at 37°C.

## Cell viability of porcine explants

For cell viability measurements, porcine explants were placed onto 13-mm, 0.2-µm pore-size membranes on 1× antimicrobial agent TSA plates and treated with e-bandages identically to the infected models, but without bacteria (Figure 1.6A–9A). Titanium wires of the working and counter electrode and the external Ag/AgCl wire were secured around the edges of Petri dishes with tape.



Tegaderm™ was used to secure the position of the e-bandage on top of the explant (Figure 1.7A and 8A). The lid was placed on the Petri dishes and secured with parafilm. Following treatment, explants were transferred to a 96-well plate with 180  $\mu\text{l}$  of DMEM and 20  $\mu\text{l}$  of PrestoBlue cell viability assay (Thermo Fisher, A13262). Explants were incubated for 3 h at 37°C in an incubator with 5% CO<sub>2</sub>, 95% air and 95% humidity, and the fluorescence measured by excitation at 535 and emission at 590 nm (Figure 1.9A, Cytation5 imaging reader, BioTek). Explant viability was normalized to initial cell viability (i.e. before treatment) and cell viability reductions by polarized e-bandages calculated as described in SI Section 1 (equations for normalized cell viability and cell viability reduction).

### ***Staphylococcus aureus* ex vivo infection model**

Three models were tested for efficacy of the e-bandage on *S. aureus*: colonization, and young and mature biofilms. Frozen stock cultures were used to grow generation 2 plates from generation 1 streak colonies on blood agar for 24 h (Trypticase™ Soy Agar II with 5% sheep blood, BD™ Cat. No. 254087). A single colony of the freshly streaked bacteria on sheep blood agar was suspended in 5 ml of TSB and incubated for 2–2.5 h at 37°C to achieve  $7.8 \pm 0.2 \log_{10}$  CFU ml<sup>-1</sup> (0.5 McFarland). For the colonization model, 10  $\mu\text{l}$  of 0.5 McFarland *S. aureus* was used to inoculate fresh explants (immediately after processing), and the e-bandages were placed and polarized 10 min later (Figure 1.6B). For the colonization model, an air incubator at 37°C was used because *S. aureus* did not grow on the no e-bandage or nonpolarized-infected explants at room temperature; all other treatments were done at room temperature. Two biofilm types were tested: young and mature. For young biofilm model, 10  $\mu\text{l}$  of 0.5 McFarland *S. aureus* was used to inoculate fresh explants and allowed to grow for 24 h. For mature biofilms, explants were inoculated with 10 or 2.5  $\mu\text{l}$  of 0.5 McFarland *S. aureus* and grown on 0.1× TSA explants for 3 days in an incubator with 5% CO<sub>2</sub>, 95% air and 95% humidity at 37°C. Every 24 h, explants were transferred to fresh 0.1× TSA plates. E-bandages were prepared and positioned identically to those of the noninfected model (Figure 1.7B and 8B). After treatment, e-bandages were rinsed with 5 ml of PBS; PBS was combined with the infected explants and membranes and vortexed for 30 s. Then, the combined solution was sonicated in a water bath for 5 min and vortexed again for 30 s. Finally, the combined solution was centrifuged for 10 min at 5000 rpm (3490×g), the supernatant discarded, and the bacterial cell pellet resuspended in 1 ml of fresh PBS. The resuspension was serially 10-fold diluted

in PBS and spread onto TSA plates for CFU quantification (Figure 1.9B). Individual colonies on the TSA plates were quantified after 24 h of growth.

### **H<sub>2</sub>O<sub>2</sub> concentration depth profiles in porcine explants**

H<sub>2</sub>O<sub>2</sub> microelectrodes were constructed similarly to those in previous work (Lewandowski & Beyenal, 2013). Briefly, an etched 50- $\mu\text{m}$  platinum wire (California Fine Wire Company Pure TC grade) was sealed inside a glass capillary (Corning 8161) using a healing coil. The tip of the sealed platinum wire was exposed and electroplated with platinum to form a 20–30  $\mu\text{m}$  ball. The microelectrodes were then dipped in a cellulose acetate membrane and dried for 24 h. To measure H<sub>2</sub>O<sub>2</sub> concentrations, the microelectrode was polarized at 0.8 V<sub>Ag/AgCl</sub> relative to an external leakless Ag/AgCl reference electrode (similar to EDAQ ET072-1). Before and after each profile, the microelectrode was calibrated using a stock solution of H<sub>2</sub>O<sub>2</sub> aliquoted into PBS from 0 to 500  $\mu\text{mol L}^{-1}$ . The calibration solution was stirred constantly. The sensitivity and limit of detection of the microelectrode were 0.01 nA  $\mu\text{mol}^{-1}$  L and 14  $\mu\text{mol L}^{-1}$  respectively. The surface of the explant/biofilm was determined using a Zeiss Stemi 2000 stereomicroscope (Carl Zeiss Microscopy) and a computer-controlled stepper motor (Physik Instrumente, part no. M230101SX) controlled by a LABVIEW script. This was used to move the microelectrode in 25- $\mu\text{m}$  increments from 200  $\mu\text{m}$  above the explant to 300  $\mu\text{m}$  below the explant/biofilm surface. A G300 Gamry potentiostat was used to measure the current response of the microelectrode (Gamry Instruments).

Immediately after an e-bandage was removed from a 48 h nonpolarized or polarized explant (infected or noninfected), the microelectrode was positioned at the surface of the explant using a stereomicroscope. The microelectrode tip was retracted by 3 mm from the surface, and 100  $\mu\text{l}$  of hydrogel added on top of the explant. The microelectrode tip was repositioned 200  $\mu\text{m}$  above the surface and polarized for 3 min to measure background current.

### **Scanning electron microscope imaging of porcine explants**

Immediately following treatment, explants were placed in 2% paraformaldehyde/2% glutaraldehyde in 0.1 M phosphate buffer and stored overnight at 4°C. To rinse the fixing solution, the explants were washed with 0.1 M phosphate buffer twice for 15 min at room temperature. Explants were dehydrated by single 15-min ethanol

treatments at concentrations of 10%, 30%, 50%, 70%, and 90% followed by two 15-min treatments at 100%. Finally, explants were critical point dried (Samdri-PVT 3B) then placed onto stubs and gold sputter-coated (Sputter Coater Technics Hummer V—Gold). A scanning electron microscope FEI Apreo and an FEI Quanta 200F microscope were used to image the explants.

## Statistical analysis

A two-sided Wilcoxon rank sum test was used to assess statistical differences between treatments; experiments with a  $p$  value  $< 0.1$  were considered significant. Due to supply limitations for pig ears, some experiments were only replicated three times. Standard deviations and means along with individual data points are presented in the figures. Triplicate experiments were performed on different days.

## RESULTS

### e-Bandages prevent *S. aureus* biofilm formation on explant

During the 48 h polarized treatment time, the no e-bandage and nonpolarized control explant models grew to  $9.4 \pm 0.3$  and  $8.6 \pm 1.0 \log_{10}$  CFU  $\text{cm}^{-2}$  respectively (Figure 2). The polarized e-bandage biofilms had an average of  $5.6 \pm 2.5 \log_{10}$  CFU  $\text{cm}^{-2}$  (reduction of  $3.0 \pm 2.3 \log_{10}$

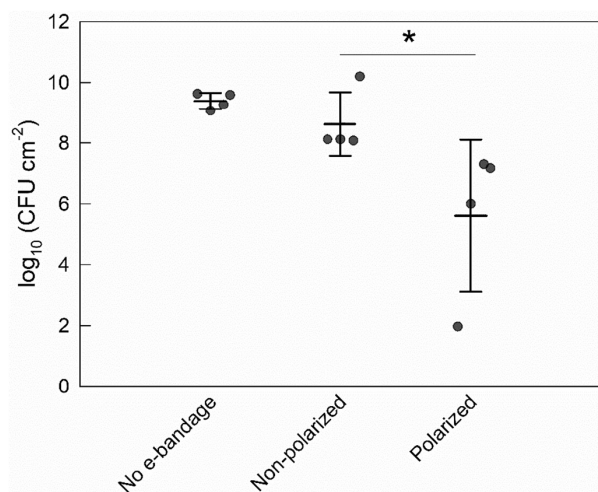


**FIGURE 2** Effect of the e-bandage on porcine explant colonization by *Staphylococcus aureus*. Treatment started immediately following explant inoculation with *S. aureus*. Data points represent individual replicates (circles), averages (horizontal lines) and standard deviations of treatment conditions. Statistical significance is indicated by a star ( $n = 4$ ).

CFU  $\text{cm}^{-2}$ ), a significant reduction compared to nonpolarized e-bandage treatment ( $p = 0.029$ ).

### e-Bandages reduce *S. aureus* cell numbers in young explant biofilms

Young biofilms reached a cell density of  $7.2 \pm 0.3 \log_{10}$  CFU  $\text{cm}^{-2}$  at treatment initiation. After treatment, explant biofilms with no e-bandages had a mean cell density of  $8.8 \pm 0.4 \log_{10}$  CFU  $\text{cm}^{-2}$ , while nonpolarized controls had a mean cell density of  $7.9 \pm 0.3 \log_{10}$  CFU  $\text{cm}^{-2}$  (Figure 3). In contrast, after polarized e-bandage treatment, the biofilm cell density was only  $2.6 \pm 2.2 \log_{10}$  CFU  $\text{cm}^{-2}$  (a reduction of  $5.4 \pm 2.0 \log_{10}$  CFU  $\text{cm}^{-2}$ ); a statistically significant reduction ( $p = 0.029$ ) compared to nonpolarized e-bandages.

### e-Bandages have limited activity against mature *S. aureus* biofilms

No e-bandage, nonpolarized and polarized explant biofilms reached cell densities of  $8.9 \pm 0.7$ ,  $9.7 \pm 0.5$  and  $8.9 \pm 0.7 \log_{10}$  CFU  $\text{cm}^{-2}$ , respectively following treatment in the  $10 \mu\text{l}$  inoculum group (Figure 4a). The cell counts in the  $10 \mu\text{l}$  inoculum mature *S. aureus* explant biofilms treated with polarized e-bandages were no different than those of controls ( $p > 0.1$ ). In contrast, in the  $2.5 \mu\text{l}$  inoculum group cell densities reached  $8.6 \pm 0.4$ ,  $9.8 \pm 0.2$  and

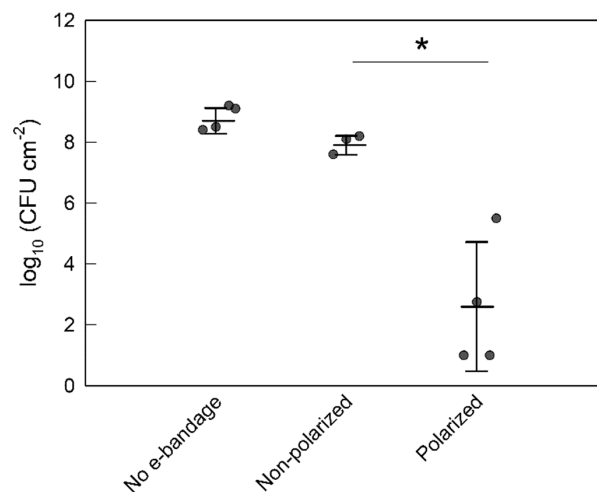


**FIGURE 3** Colony-forming units of *Staphylococcus aureus* biofilms grown on porcine explants after treatment with the e-bandage for biofilm removal of young biofilms. Treatment started 24 h after explant inoculation with *S. aureus*. Data points represent individual replicates (circles), averages (horizontal lines) and standard deviations of treatment conditions. Statistical significance is indicated by a star ( $n = 4$ ).

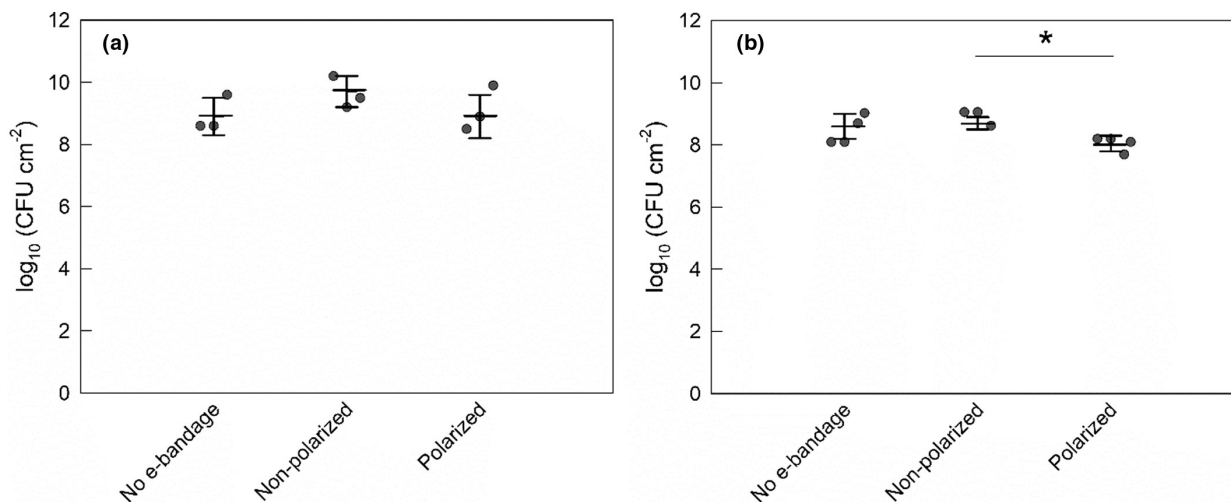


**FIGURE 4** Colony-forming units of *Staphylococcus aureus* biofilms grown on pig ear explants after treatment with the e-bandages. Treatment started 3 days after explant inoculation with *S. aureus* inoculum of (a) 10  $\mu\text{l}$  and (b) 2.5  $\mu\text{l}$ . Data points represent individual replicates (circles), averages (horizontal lines) and standard deviations of treatment conditions. Statistical significance is indicated by a star ( $n \geq 3$ ).

$9.1 \pm 0.3 \log_{10} \text{CFU cm}^{-2}$  for no e-bandage, nonpolarized and polarized e-bandage biofilms respectively (Figure 4b); in this group, mature *S. aureus* explant biofilms were reduced by  $0.7 \pm 0.2 \log_{10} \text{CFU cm}^{-2}$  by polarized treatment ( $p = 0.029$ ).

### Scanning electron microscopy imaging of infected and noninfected explants

Electron microscopy images of noninfected and infected explants with no e-bandages, nonpolarized e-bandages and polarized e-bandages are shown in SI Section 2. Electron microscopy images of the no e-bandage noninfected (Figures S1A and S2A) and infected (Figure S3A and S4A) explants showed well-defined dermis fibres. Sphere-shaped *S. aureus* cells were observed on the surface of the infected explants. The 0-day infected explants were sparingly covered with *S. aureus* cells, while the 3-day explants had greater coverage of the surface. With nonpolarized e-bandage explants (Figures S1B, S2B, S3B and S4B), the dermis fibres were still well defined and additional structures were observed on the tissue surface, likely dried hydrogel remnants. Unlike tissues not exposed to e-bandages or exposed to nonpolarized explants, noninfected (Figures S1C and S2C) and infected (Figures S3C and S4C) tissues exposed to polarized e-bandages showed morphological changes. The fibres appeared to be damaged and crushed together and, in some locations, a crust was observed on the tissue. When comparing *S. aureus* cells not exposed to an e-bandage or exposed to nonpolarized e-bandages, tissue exposed to polarized e-bandages had cells that appeared to rest on the surface of the tissue

rather than weaving through the fibres. No morphological changes in *S. aureus* cells were observed after polarized treatment.

### H<sub>2</sub>O<sub>2</sub> concentration profiles

H<sub>2</sub>O<sub>2</sub> was not measurable in explants immediately after processing or in nonpolarized explants (Figure 5a,b), whether infected or noninfected. For infected explants, H<sub>2</sub>O<sub>2</sub> was measured in hydrogel to a concentration of  $\sim 150 \mu\text{mol L}^{-1}$  (Figure 5a). After polarized e-bandage treatment, H<sub>2</sub>O<sub>2</sub> was measurable inside both *S. aureus* infected and noninfected explant tissue to at least 300  $\mu\text{m}$  below the surface. H<sub>2</sub>O<sub>2</sub> was measured in the concentration range of 120–250  $\mu\text{mol L}^{-1}$  in hydrogel and tissue of infected explants. In the noninfected but polarized group, H<sub>2</sub>O<sub>2</sub> was detected in the hydrogel and explant tissue between 150 and 275  $\mu\text{mol L}^{-1}$  (Figure 5b). For both infected and noninfected explant profiles, the H<sub>2</sub>O<sub>2</sub> concentration decreased as the microelectrode tip moved further into the tissue.

### Eukaryotic cell viability

There was no statistical difference between the viability of 0-day explants exposed to no e-bandages and nonpolarized e-bandages ( $p > 0.1$ ). There was a 44% average reduction in normalized cell viability between 0-day explants exposed to polarized and nonpolarized e-bandages, but the difference that was not statistically significant ( $p > 0.1$ ) (Figure 6a). Viability of 3-day explants exposed to

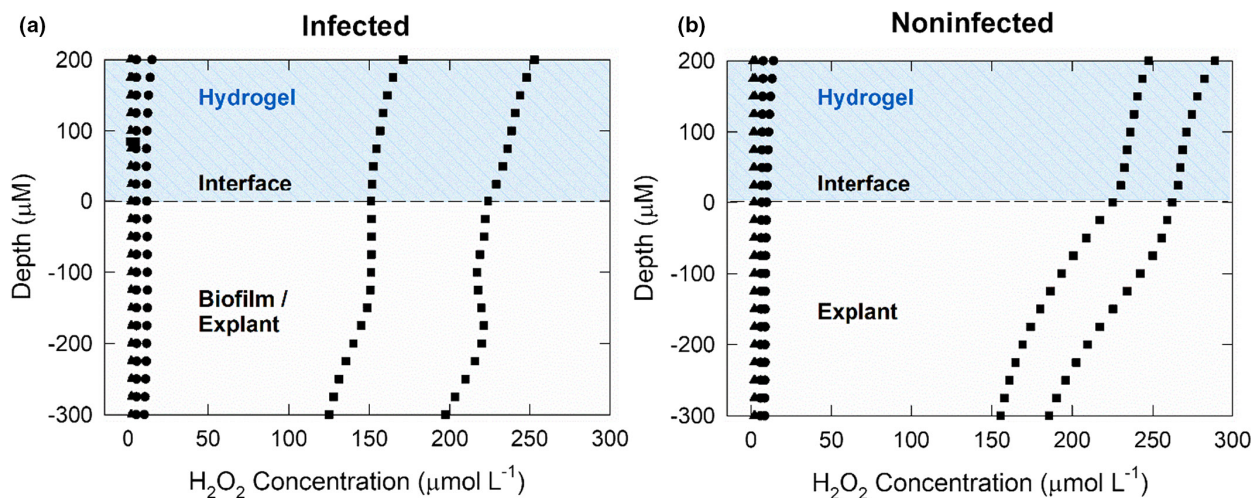


**FIGURE 5** Depth profiles of the concentration of H<sub>2</sub>O<sub>2</sub> generated by polarized e-bandages in explant tissue and overlying hydrogel: (a) infected and (b) noninfected explants. ▲ explant at baseline with no treatment; ● explant after exposure to nonpolarized e-bandage for 48 h and ■ explant exposed to a polarized e-bandage for 48 h.

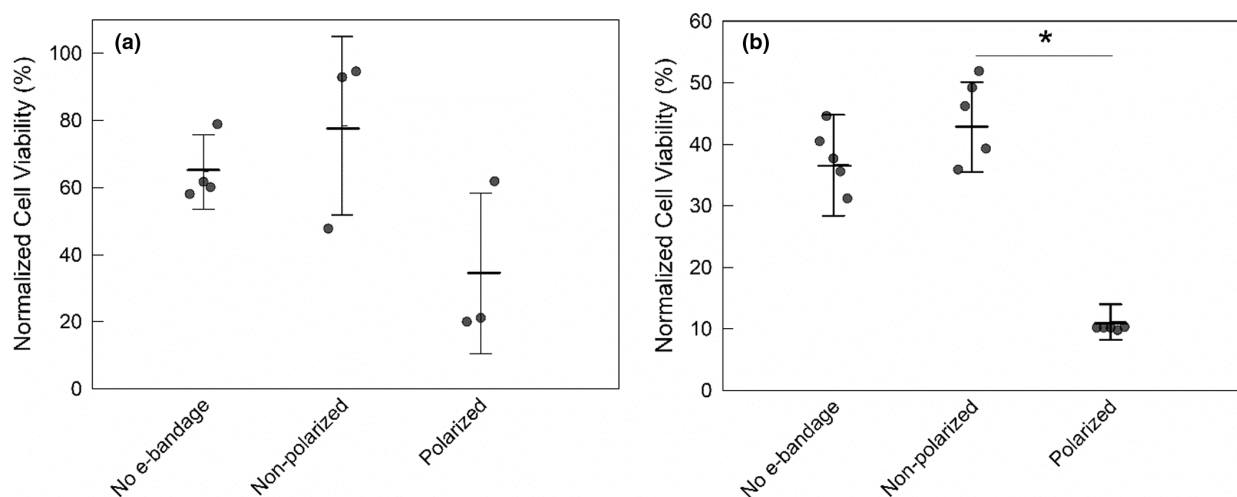


**FIGURE 6** Effect of e-bandage on cell viability of noninfected explants. Normalized cell viability of explants treated with no e-bandage, or nonpolarized or polarized e-bandages at (a)  $t = 0$  and (b)  $t = 3$  days. Data points represent individual replicates (circles), averages (horizontal lines) and standard deviations of treatment conditions. Statistical significance is indicated by a star ( $n \geq 3$ ).

polarized e-bandages decreased by 32% compared to nonpolarized explant ( $p = 0.001$ ) (Figure 6b).

## DISCUSSION

Biofilm infections are difficult to treat using systemic and topical administration of antibiotics because of the rise of antibiotic-resistant micro-organisms and because of biofilm-specific antibiotic tolerance. The *in situ* electrochemical generation of biocides such as H<sub>2</sub>O<sub>2</sub> is a potential approach for managing wound biofilm infections. Two devices have been developed based on an electrochemical

H<sub>2</sub>O<sub>2</sub> concept: e-scaffolds were developed to assess activity against biofilms grown in liquid growth media, and then e-bandages were developed to treat agar membrane (and eventually wound) biofilms. e-Scaffolds demonstrated anti-biofilm efficacy against mono-, dual- and tri-species bacterial and fungal biofilms, without significant toxicity to host tissue in an *ex vivo* porcine explant model (Raval et al., 2019, 2020; Raval, Flurin, et al., 2021; Sultana et al., 2015, 2016). In addition, it was suggested that H<sub>2</sub>O<sub>2</sub> generation by the electrode was the dominant mechanism of action (Sultana et al., 2015). With the e-bandage, an agar membrane biofilm model was used to simulate physical properties of the wound bed and validate the



technology prior to animal testing. Polarized e-bandages were active against mono- and dual-species bacterial and yeast biofilms (Raval et al., 2022; Raval, Mohamed, et al., 2021). In this work, validation was extended to assessment of e-bandages against *ex vivo* biofilms grown on porcine explants.

Porcine explant models were used because of the structural similarity of pig to human skin and cost-effectiveness of the materials (Sullivan et al., 2001). The use of porcine explant models for initial assessment of efficacy and toxicity of potential antibacterial agents has been reported previously. For example, agar explant models were designed to assess toxicity and efficacy of multiple wound cleansers (McMahon et al., 2020; Roche et al., 2019). A similar model was adopted in this work to test the efficacy and toxicity of the e-bandage. The concentration of agar was increased and the concentration of antibiotics varied to address specific requirements. Increasing the agar concentration provided a stronger platform for physically supporting e-bandages. Using full strength antibiotic (1×) prevented noninfected explants from being contaminated before e-bandage treatment, while 0.1× antibiotic was suitable for allowing biofilms to grow on explants but keeping the biofilm within the boundary of the polycarbonate membrane. Cleaning of porcine tissue during processing was also modified from previous literature. Tissue has often been sterilized with chlorine gas before being infected with bacteria, but it was found that a surgical cleaning procedure with betadine and ethanol was adequate to prevent contamination with other pathogens (Phillips et al., 2015; Roche et al., 2019; Yang et al., 2013). In the end, a modified explant biofilm model was used to assess e-bandage antimicrobial activity and toxicity, and transport of H<sub>2</sub>O<sub>2</sub> into explant tissue.

As all *ex vivo* models are limited by tissue viability being controlled by external conditions, such as the temperature, humidity and suspension medium, the modified explant biofilm model was likely more susceptible to external stresses than actual wounds. Natural biocides that are produced during an immune response to infection are not generated in *ex vivo* models (Halliwell, Clement, & Long, 2000). Lack of immune response means that any prevention of infection or biofilm removal in the evaluated system was a result of the H<sub>2</sub>O<sub>2</sub> produced by the e-bandage. The effect on colonization of the e-bandage was studied for the first time with promising results. The e-bandage prevented *S. aureus* colonization of explants (Figure 2), and was active against established young *S. aureus* biofilms (Figure 3). *S. aureus* is most susceptible to treatment during the first 24 h when it is developing a biofilm (Alves et al., 2018). The e-bandage removed 5.4 log<sub>10</sub> CFU cm<sup>-2</sup> of a young *S. aureus* biofilm cells. Mature biofilms were more refractory to treatment, as expected,

likely because of the complex interaction between *S. aureus* and the explant. As biofilms mature, EPS content increases, cell numbers increase and the biofilm becomes more resilient against external challenges. The activity of H<sub>2</sub>O<sub>2</sub> was studied on biofilm and planktonic phenotypes of 27 isolates of eight bacterial species (Raval, Flurin, et al., 2021). H<sub>2</sub>O<sub>2</sub>-generating e-scaffolds had reduced activity against biofilms compared to their activity against planktonic cells. A possible reason for lower efficacy against mature compared to young biofilms, is that after 3 days, *S. aureus* cells are found hundreds of micrometres below the tissue surface (Yang et al., 2013). Another study found that *S. aureus* cells burrowed several hundred micrometres into tissue and mucosa (Cantero et al., 2013; Nakatsuji et al., 2016). Although penetration of *S. aureus* cells into the dermis was not observed in all explant experiments, the action of burrowing into tissue may be a reason that mature biofilms were less affected by e-bandages than young biofilms (Lone et al., 2015). Another reason for the reduced efficacy could be nonspecific reactions between H<sub>2</sub>O<sub>2</sub>, the EPS, or its components. For example, H<sub>2</sub>O<sub>2</sub> was found to degrade natural polysaccharides (Ofoedu et al., 2021). EPS is comprised of many other components including dead cells, proteins, and extracellular DNA (Denkhaus et al., 2007; Stewart, 1996). In the absence of antibiotic therapies, the e-bandage facilitated a limited reduction of mature biofilms (Figure 4). The efficacy of the e-bandage could be due to transport of H<sub>2</sub>O<sub>2</sub> into the tissue during treatment.

Several methods for measuring transport of H<sub>2</sub>O<sub>2</sub> through tissue have been described. Nanosensors were used to detect H<sub>2</sub>O<sub>2</sub> in *ex vivo* cells by extrapolating the reaction of H<sub>2</sub>O<sub>2</sub> with Prussian white forming Prussian blue (Marquitan et al., 2016). H<sub>2</sub>O<sub>2</sub> transport was also measured using the reaction of Prussian white to blue to image the explant surface (Jankovskaja et al., 2020). A synthesized H<sub>2</sub>O<sub>2</sub>-response analogue for electrochemically monitoring H<sub>2</sub>O<sub>2</sub> permeation through tissue was tested (Yik-Sham Chung et al., 2018). Other electrochemical techniques, such as microelectrodes, can be used to measure concentration profiles in explant experiments and biofilms. Microelectrode profiles for measuring changes in pH and dissolved oxygen concentrations were conducted on uninfected and *S. aureus* infected explant tissue several hundreds of microns below the surface (Lone et al., 2015). H<sub>2</sub>O<sub>2</sub> concentration profiles have also been measured using microelectrodes in *P. aeruginosa* biofilms (Stewart et al., 2000). The generation of H<sub>2</sub>O<sub>2</sub> by the e-bandage was verified under abiotic conditions using microelectrodes (Mohamed et al., 2021). The concentration of H<sub>2</sub>O<sub>2</sub> increased as polarizing time increased, reaching local concentrations up to 320 μmol L<sup>-1</sup>. In this work, microelectrodes were used to measure H<sub>2</sub>O<sub>2</sub> directly above

and below the surface of explants and explant biofilms (Figure 5).

Two important observations were made based on the  $H_2O_2$  profiles. First,  $H_2O_2$  was measured in fresh hydrogel added atop the explant after the e-bandage was removed and prior to  $H_2O_2$  measurement. This indicates that  $H_2O_2$  likely diffused from the explant itself following removal of the e-bandage, which shows that  $H_2O_2$  was not bound to tissue biomolecules. Second,  $H_2O_2$  concentration in the tissue was highest at the hydrogel-explant or hydrogel-biofilm surface (Figure 5).  $H_2O_2$  generated by e-bandages diffuses toward the explant surface and is then transported into tissue. As the  $H_2O_2$  permeates throughout the tissue, the concentration decreases. The decrease in concentration may be a result of hindered transport into tissue because of nonspecific reactions. Higher  $H_2O_2$  concentrations in noninfected explants could be explained by reduced consumption of  $H_2O_2$  due to reactions with biofilm cells, EPS and  $H_2O_2$ -degrading enzymes.  $H_2O_2$  is expected to be consumed as biofilm is removed from the infected explant. It is expected that electrochemical  $H_2O_2$  generation will decrease pH. However, the hydrogel contains a buffer which is expected to limit pH changes (until buffering capacity is depleted). If a pH change happens, it will vary by distance from the electrode surface. It has been shown that pH in methicillin-resistant *Staphylococcus aureus* (MRSA)-infected tissue drops from 7 to 5. This indicates MRSA biofilm cause a pH decrease on the tissue and MRSA can survive at low pH (Wang et al., 2015). In addition, previously, we reported pH changes near working electrode surface measured using a microelectrode and found no significant pH change (Sultana et al., 2015). Lastly, we measured average pH of the hydrogel after 48 hours using a pH paper and it was between 5 and 6.

$H_2O_2$  transport into the explant is expected to affect biofilm removal and tissue viability. A review of effects of  $H_2O_2$  on the human body found that toxicity can occur at as little as  $50\mu\text{molL}^{-1}$ , depending on exposure time and location (Gülden et al., 2010; Halliwell, Clement, & Long, 2000). During the natural immune response,  $H_2O_2$  is formed from reactive oxygen species and targets bacteria and mammalian cells alike (Halliwell, Clement, & Long, 2000; Halliwell, Clement, Ramalingam, et al., 2000).  $H_2O_2$  may contribute to loosening and rupture of tissue fibres, resulting in what appeared to be a crust over the surface of the explants (SI Section 2) (Liu et al., 2014). A reduction in viability in the *ex vivo* porcine explant biofilm model was observed (Figure 6). An important limitation is that *ex vivo* tissue cannot regenerate or protect cells from oxidative stress. Cells are equipped with enzymes such as catalase, glutathione peroxidase, superoxide dismutase and thioredoxin-linked systems to eliminate  $H_2O_2$  and prevent the formation of reactive oxygen radicals (OH $\cdot$ )

(Mahaseth & Kuzminov, 2017). In animal models and clinical applications, where the tissue has multiple methods of eliminating  $H_2O_2$ , such as using enzymes to prevent formation of OH $\cdot$  and using myeloperoxidase to produce other antimicrobial oxidants, cell viability is expected to be less affected by the e-bandage (Halliwell, Clement, Ramalingam, et al., 2000; Paumann-Page et al., 2013). Both chemical oxidants and some metabolic products from infections can result in apoptosis and damage to the surrounding tissue of a wound.

A limitation of the *ex vivo* model was the inability to study the impact of the e-bandage on wound healing. Infections are a critical factor impairing wound healing (Guo & Dipietro, 2010). Infections alter the balance of inflammation, compete for oxygen and inhibit the inflammatory phase of wound healing, preventing epithelialization (Armstrong, 2021). Documented causes of *S. aureus* causing apoptosis in human tissue and epithelial cells through virulence factor production support the idea that infections slow or inhibit wound healing (Haslinger-Löffler et al., 2005; Nakatsuji et al., 2016). *S. aureus* infections also cause alkaline pH and decreased oxygen concentrations at wound surfaces (Lone et al., 2015). Therefore, e-bandage treatment may result in improved wound healing rates due to the removal/reduction of *S. aureus* biofilms.

The results of the *ex vivo* porcine explant biofilm model presented here support that  $H_2O_2$ -producing e-bandages slowed down *S. aureus* biofilm colonization and reduced young *S. aureus* biofilms. E-bandage efficacy against mature biofilms was limited.  $H_2O_2$  was shown to penetrate both noninfected and infected explants and e-bandages were shown to reduce eukaryotic cell viability to some extent. Future studies will focus on evaluating the efficacy of the e-bandage in *in vivo* models.

## ACKNOWLEDGEMENTS

Research reported in this publication was supported by the National Institute of Allergy and Infectious Diseases of the National Institutes of Health under award number R01AI091594. The content is solely the responsibility of the authors and does not necessarily represent the official views of the National Institutes of Health. The authors thank C&L Locker in Moscow, ID and the University of Idaho Beef Center for providing the porcine materials. Electron microscopy, sample preparation protocols, and support were provided by the Washington State University Franceschi Microscopy and Imaging Center.


## CONFLICT OF INTEREST

H.B. holds a patent (US20180207301A1), 'Electrochemical reduction or prevention of infections', which refers to the electrochemical scaffold described herein. R.P. reports

grants from ContraFect, TenNor Therapeutics Limited, and BioFire. R.P. is a consultant to Curetis, Specific Technologies, Next Gen Diagnostics, PathoQuest, Selux Diagnostics, 1928 Diagnostics, PhAST, Torus Biosystems, Day Zero Diagnostics, Mammoth Biosciences, CARB-X, and Qvella; monies are paid to Mayo Clinic. Mayo Clinic and R.P. have relationships with Adaptive Phage Therapeutics and Pathogenomix. R.P. is also a consultant to Netflix. In addition, R.P. has a patent on *Bordetella pertussis/parapertussis* PCR issued, a patent on a device/method for sonication with royalties paid by Samsung to Mayo Clinic, and a patent on an anti-biofilm substance issued. R.P. receives honoraria from the NBME, Up-to-Date and the Infectious Diseases Board Review Course.

## ORCID


Gretchen Tibbits  <https://orcid.org/0000-0002-4285-2258>

Abdelrhman Mohamed  <https://orcid.org/0000-0003-2132-0487>

Suzanne Gelston  <https://orcid.org/0000-0001-6853-8067>

Laure Flurin  <https://orcid.org/0000-0001-5687-1081>

Yash S. Raval  <https://orcid.org/0000-0003-1161-4000>

Kerryl Greenwood-Quaintance  <https://orcid.org/0000-0003-3760-4310>

Robin Patel  <https://orcid.org/0000-0001-6344-4141>

Haluk Beyenal  <https://orcid.org/0000-0003-3931-0244>

## REFERENCES

- Allen J. Bard, L.R.F. (2001) *Electrochemical methods: fundamentals and applications*. New York: Wiley.
- Alves, D.R., Booth, S.P., Scavone, P., Schellenberger, P., Salvage, J., Dedi, C. et al. (2018) Development of a high-throughput *ex-vivo* burn wound model using porcine skin, and its application to evaluate new approaches to control wound infection. *Frontiers in Cellular and Infection Microbiology*, 8, 8.
- Anderl, J.N., Franklin, M.J. & Stewart, P.S. (2000) Role of antibiotic penetration limitation in *Klebsiella pneumoniae* biofilm resistance to ampicillin and ciprofloxacin. *Antimicrobial Agents and Chemotherapy*, 44, 1818–1824.
- Armstrong, D.G.M.A.J. (2021) *Risk factors for impaired wound healing and wound complications*. In: Berman, R.S., Eidt, J.F., Mills, J.L. & Cochran, A. (Eds.). UpToDate.com.
- Cantero, D., Cooksley, C., Jardeleza, C., Bassiouni, A., Jones, D., Wormald, P.J. et al. (2013) A human nasal explant model to study *Staphylococcus aureus* biofilm in vitro. *International Forum of Allergy & Rhinology*, 3, 556–562.
- Davenport, E.K., Call, D.R. & Beyenal, H. (2014) Differential protection from tobramycin by extracellular polymeric substances from *Acinetobacter baumannii* and *Staphylococcus aureus* biofilms. *Antimicrobial Agents and Chemotherapy*, 58, 4755–4761.
- Denkhaus, E., Meisen, S., Telgheder, U. & Wingender, J. (2007) Chemical and physical methods for characterisation of biofilms. *Microchimica Acta*, 158, 1–27.
- Devaraj, A., Buzzo, J.R., Mashburn-Warren, L., Gloag, E.S., Novotny, L.A., Stoodley, P. et al. (2019) The extracellular DNA lattice of bacterial biofilms is structurally related to Holliday junction recombination intermediates. *Proceedings of the National Academy of Sciences of the United States of America*, 116, 25068–25077.
- Dowd, S.E., Delton Hanson, J., Rees, E., Wolcott, R.D., Zischau, A.M., Sun, Y. et al. (2011) Survey of fungi and yeast in polymicrobial infections in chronic wounds. *Journal of Wound Care*, 20, 40–47.
- Finnegan, M., Linley, E., Denyer, S.P., McDonnell, G., Simons, C. & Maillard, J.Y. (2010) Mode of action of hydrogen peroxide and other oxidizing agents: differences between liquid and gas forms. *The Journal of Antimicrobial Chemotherapy*, 65, 2108–2115.
- Gülden, M., Jess, A., Kammann, J., Maser, E. & Seibert, H. (2010) Cytotoxic potency of H<sub>2</sub>O<sub>2</sub> in cell cultures: impact of cell concentration and exposure time. *Free Radical Biology & Medicine*, 49, 1298–1305.
- Guo, S. & Dipietro, L.A. (2010) Factors affecting wound healing. *Journal of Dental Research*, 89, 219–229.
- Gupta, P., Sarkar, S., Das, B., Bhattacharjee, S. & Tribedi, P. (2016) Biofilm, pathogenesis and prevention—a journey to break the wall: a review. *Archives of Microbiology*, 198, 1–15.
- Halliwell, B., Clement, M.V. & Long, L.H. (2000) Hydrogen peroxide in the human body. *FEBS Letters*, 486, 10–13.
- Halliwell, B., Clement, M.V., Ramalingam, J. & Long, L.H. (2000) Hydrogen peroxide. Ubiquitous in cell culture and in vivo? *IUBMB Life*, 50, 251–257.
- Hampton, M.B., Kettle, A.J. & Winterbourn, C.C. (1998) Inside the neutrophil phagosome: oxidants, myeloperoxidase, and bacterial killing. *Blood*, 92, 3007–3017.
- Haslinger-Löffler, B., Kahl, B.C., Grundmeier, M., Strangfeld, K., Wagner, B., Fischer, U. et al. (2005) Multiple virulence factors are required for *Staphylococcus aureus*-induced apoptosis in endothelial cells. *Cellular Microbiology*, 7, 1087–1097.
- Højby, N., Ciofu, O., Johansen, H.K., Song, Z.J., Moser, C., Jensen, P. et al. (2011) The clinical impact of bacterial biofilms. *International Journal of Oral Science*, 3, 55–65.
- Jankovskaja, S., Labrousse, A., Prévaud, L., Holmqvist, B., Brinte, A., Engblom, J. et al. (2020) Visualisation of H<sub>2</sub>O<sub>2</sub> penetration through skin indicates importance to develop pathway-specific epidermal sensing. *Mikrochimica Acta*, 187, 656.
- Kowal, J., Tkach, M. & Théry, C. (2014) Biogenesis and secretion of exosomes. *Current Opinion in Cell Biology*, 29, 116–125.
- Lewandowski, Z. & Beyenal, H. (2013) *Fundamentals of biofilm research*, 2nd edition. Boca Raton, FL, USA: Taylor & Francis.
- Liu, X., Jiang, Y., He, H. & Ping, W. (2014) Hydrogen peroxide-induced degradation of type I collagen fibers of tilapia skin. *Food Structure*, 2, 41–48.
- Lone, A.G., Atci, E., Renslow, R., Beyenal, H., Noh, S., Fransson, B. et al. (2015) *Staphylococcus aureus* induces hypoxia and cellular damage in porcine dermal explants. *Infection and Immunity*, 83, 2531–2541.
- Mahaseth, T. & Kuzminov, A. (2017) Potentiation of hydrogen peroxide toxicity: from catalase inhibition to stable DNA-iron complexes. *Mutation Research, Reviews in Mutation Research*, 773, 274–281.
- Marquitan, M., Clausmeyer, J., Actis, P., Cordoba, A.L., Korchev, Y., Mark, M.D. et al. (2016) Intracellular hydrogen peroxide detection



- with functionalised nanoelectrodes. *ChemElectroChem*, 3, 2125–2129.
- McMahon, R.E., Salamone, A.B., Poleon, S., Bionda, N. & Salamone, J.C. (2020) Efficacy of wound cleansers on wound-specific organisms using *in vitro* and *ex vivo* biofilm models. *Wound Management & Prevention*, 66, 31–42.
- Metcalfe, D.G. & Bowler, P.G. (2013) Biofilm delays wound healing: a review of the evidence. *Burns & Trauma*, 1, 5–12.
- Mohamed, A., Anoy, M.M.I., Tibbits, G., Raval, Y.S., Flurin, L., Greenwood-Quaintance, K.E. et al. (2021) Hydrogen peroxide-producing electrochemical bandage controlled by a wearable potentiostat for treatment of wound infections. *Biotechnology and Bioengineering*, 118, 2815–2821.
- Nakatsuji, T., Chen, T.H., Two, A.M., Chun, K.A., Narala, S., Geha, R.S. et al. (2016) *Staphylococcus aureus* exploits epidermal barrier defects in atopic dermatitis to trigger cytokine expression. *The Journal of Investigative Dermatology*, 136, 2192–2200.
- Ofoedu, C.E., You, L., Osuji, C.M., Iwouno, J.O., Kabuo, N.O., Ojukwu, M. et al. (2021) Hydrogen peroxide effects on natural-sourced Polysaccharides: free radical formation/production, degradation process, and reaction mechanism-A critical synopsis. *Food*, 10, 699.
- Paumann-Page, M., Furtmüller, P.G., Hofbauer, S., Paton, L.N., Obinger, C. & Kettle, A.J. (2013) Inactivation of human myeloperoxidase by hydrogen peroxide. *Archives of Biochemistry and Biophysics*, 539, 51–62.
- Percival, S.L., Hill, K.E., Williams, D.W., Hooper, S.J., Thomas, D.W. & Costerton, J.W. (2012) A review of the scientific evidence for biofilms in wounds. *Wound Repair and Regeneration*, 20, 647–657.
- Phillips, P.L., Yang, Q., Davis, S., Sampson, E.M., Azeke, J.I., Hamad, A. et al. (2015) Antimicrobial dressing efficacy against mature *Pseudomonas aeruginosa* biofilm on porcine skin explants. *International Wound Journal*, 12, 469–483.
- Raval, Y.S., Flurin, L., Mohamed, A., Greenwood-Quaintance, K.E., Beyenal, H. & Patel, R. (2021) *In vitro* antibacterial activity of hydrogen peroxide and hypochlorous acid, including that generated by electrochemical scaffolds. *Antimicrobial Agents and Chemotherapy*, 65, e01966-01920.
- Raval, Y.S., Mohamed, A., Flurin, L., Mandrekar, J.N., Greenwood-Quaintance, K.E., Beyenal, H. et al. (2021) Hydrogen-peroxide generating electrochemical bandage is active *in vitro* against mono- and dual-species biofilms. *Biofilms*, 3, 100055.
- Raval, Y.S., Mohamed, A., Mandrekar, J.N., Fisher, C., Greenwood-Quaintance, K.E., Beyenal, H. et al. (2022) *In vitro* antibiogram activity of hydrogen peroxide-generating electrochemical bandage against yeast biofilms. *Antimicrobial Agents and Chemotherapy*, 66, e0179221.
- Raval, Y.S., Mohamed, A., Song, J., Greenwood-Quaintance, K.E., Beyenal, H. & Patel, R. (2020) Hydrogen peroxide-generating electrochemical scaffold activity against trispecies biofilms. *Antimicrobial Agents and Chemotherapy*, 64, e02332–e02319.
- Raval, Y.S., Mohamed, A., Zmuda, H.M., Patel, R. & Beyenal, H. (2019) Hydrogen-peroxide-generating electrochemical scaffold eradicates methicillin-resistant *Staphylococcus aureus* biofilms. *Global Challenges*, 3, 1800101.
- Roberts, A.E.L., Powell, L.C., Pritchard, M.F., Thomas, D.W. & Jenkins, R.E. (2019) Anti-pseudomonad activity of manuka honey and antibiotics in a specialized *ex vivo* model simulating cystic fibrosis lung infection. *Frontiers in Microbiology*, 10, 869.
- Roche, E.D., Woodmansey, E.J., Yang, Q., Gibson, D.J., Zhang, H. & Schultz, G.S. (2019) Cadexomer iodine effectively reduces bacterial biofilm in porcine wounds *ex vivo* and *in vivo*. *International Wound Journal*, 16, 674–683.
- Sen, C.K. (2019) Human wounds and its burden: an updated compendium of estimates. *Advances in Wound Care (New Rochelle)*, 8, 39–48.
- Shrout, J.D., Tolker-Nielsen, T., Givskov, M. & Parsek, M.R. (2011) The contribution of cell-cell signaling and motility to bacterial biofilm formation. *MRS Bulletin*, 36, 367–373.
- Stewart, P.S. (1996) Theoretical aspects of antibiotic diffusion into microbial biofilms. *Antimicrobial Agents and Chemotherapy*, 40, 2517–2522.
- Stewart, P.S., Roe, F., Rayner, J., Elkins, J.G., Lewandowski, Z., Ochsner, U.A. et al. (2000) Effect of catalase on hydrogen peroxide penetration into *Pseudomonas aeruginosa* biofilms. *Applied and Environmental Microbiology*, 66, 836–838.
- Sullivan, T.P., Eaglstein, W.H., Davis, S.C. & Mertz, P. (2001) The pig as a model for human wound healing. *Wound Repair and Regeneration*, 9, 66–76.
- Sultana, S.T., Atci, E., Babauta, J.T., Mohamed Falghoush, A., Snekvik, K.R., Call, D.R. et al. (2015) Electrochemical scaffold generates localized, low concentration of hydrogen peroxide that inhibits bacterial pathogens and biofilms. *Scientific Reports*, 5, 14908.
- Sultana, S.T., Call, D.R. & Beyenal, H. (2016) Eradication of *Pseudomonas aeruginosa* biofilms and persister cells using an electrochemical scaffold and enhanced antibiotic susceptibility. *npj Biofilms and Microbiomes*, 2, 2.
- Uruen, C., Chopo-Escuin, G., Tommassen, J., Mainar-Jaime, R.C. & Arenas, J. (2021) Biofilms as promoters of bacterial antibiotic resistance and tolerance. *Antibiotics (Basel)*, 10, 3.
- Valadi, H., Ekström, K., Bossios, A., Sjöstrand, M., Lee, J.J. & Lötvall, J.O. (2007) Exosome-mediated transfer of mRNAs and microRNAs is a novel mechanism of genetic exchange between cells. *Nature Cell Biology*, 9, 654–659.
- Wang, F., Raval, Y., Tzeng, T.-R.J. & Anker, J.N. (2015) X-ray excited luminescence chemical imaging of bacterial growth on surfaces implanted in tissue. *Advanced Healthcare Materials*, 4, 903–910.
- Yang, Q., Larose, C., Della Porta, A.C., Schultz, G.S. & Gibson, D.J. (2017) A surfactant-based wound dressing can reduce bacterial biofilms in a porcine skin explant model. *International Wound Journal*, 14, 408–413.
- Yang, Q., Phillips, P.L., Sampson, E.M., Progulske-Fox, A., Jin, S., Antonelli, P. et al. (2013) Development of a novel *ex vivo* porcine skin explant model for the assessment of mature bacterial biofilms. *Wound Repair and Regeneration*, 21, 704–714.
- Yik-Sham Chung, C., Timblin, G.A., Saijo, K. & Chang, C.J. (2018) Versatile histochemical approach to detection of hydrogen peroxide in cells and tissues based on puromycin staining. *Journal of the American Chemical Society*, 140, 6109–6121.
- Zmuda, H.M., Mohamed, A., Raval, Y.S., Call, D.R., Schuetz, A.N., Patel, R. et al. (2020) Hypochlorous acid-generating



electrochemical scaffold eliminates *Candida albicans* biofilms.  
*Journal of Applied Microbiology*, 129, 776–786.

### SUPPORTING INFORMATION

Additional supporting information can be found online in the Supporting Information section at the end of this article.

**How to cite this article:** Tibbits, G., Mohamed, A., Gelston, S., Flurin, L., Raval, Y.S. & Greenwood-Quaintance, K. et al. (2022) Efficacy and toxicity of hydrogen peroxide producing electrochemical bandages in a porcine explant biofilm model. *Journal of Applied Microbiology*, 133, 3755–3767. Available from: <https://doi.org/10.1111/jam.15812>